











Design and Characterization of Porous Titanium Scaffolds: An Alternative for Dental Implant

Danaysi Mena¹(✉) , Paloma Trueba¹ , Luisa Marleny Rodríguez-Albelo¹ ,
Ana Alcudia² , Francisco J. García-García¹ , Paula Navarro^{1,3} ,
Julio E. de la Rosa¹ , and Yadir Torres¹ 

¹ Departamento de Ingeniería y Ciencia de los Materiales y del Transporte, Escuela Politécnica Superior, Universidad de Sevilla, Sevilla, Spain

dmena@us.es

² Departamento de Química Orgánica y Farmacéutica, Facultad de Farmacia, Universidad de Sevilla, Sevilla, Spain

³ Departamento de Tecnología Electrónica, Escuela Superior de Ingeniería Informática, Universidad de Sevilla, Sevilla, Spain

Abstract. The demand for dental implants is increasing, although there is a wide variety of implants currently available in the market, it is necessary to implement improvements in their design and/or the selection of materials used. The development of biomimetic and bioactive Ti scaffolds for bone regeneration is necessary. In this context, this article proposes the design, manufacture and characterization of a porous titanium implant with the aim of eliminating some of the deficiencies found in commercially available titanium implants. Stress-shielding and the lack of osseointegration or bacterial infection are still some limitations to solve. Porous samples were produced using conventional Powder Metallurgy (PM) and the space holder (SH) technique. Ammonium bicarbonate particles were used as spacers in size ranges of 100–200 μm . The porosity and surface characterization were performed by Archimedes' method and image analysis, while the mechanical behavior was analyzed by micro-mechanical testing. After that, the micromachining protocol of the implant is carried out. Substrates were chemically etched by immersion in fluorhydric acid at different times (15 s; 60 s and 125 s) to achieve a suitable surface roughness with biofunctional balance. Results showed that it is possible to obtain a desired longitudinal gradient. The optimized method described in this work suggests that it is a reasonable candidate for the development of dental implants with a good balance between reduced stress shielding and adequate mechanical strength.

Keywords: dental implant · commercially pure titanium · porosity

1 Introduction

At present, dental implants are the most effective treatment for edentulism. Researchers worldwide are searching for substantial improvements to the available commercial implants, with the primary goal of addressing their main deficiencies. Titanium and

its alloys are the most used metallic material for their fabrication, due to their biocompatibility and osseointegration capacity. However, one of its weaknesses is the difference stiffness (Young's modulus) between the implant (105–110 GPa) and the cortical bone (20–25 GPa), which causes stress shielding phenomenon [1]. As a result, bone resorption around the dental implant is manifested [2]. In addition, the titanium osseointegration process remains insufficient to generate a resistant interface between the bone and the implant, leading to device micromovements. Furthermore, peri-implantitis still affects the hard and soft tissues surrounding the dental implant. Oral microbiota is an active community that forms symbiotic associations with bacteria [3]. To address these drawbacks, this work proposes the fabrication of a preform designed with longitudinal porosity through the conventional PM and space-holder technique [4]. Our research group has optimized the parameters for processing routes used to obtain porous titanium substrates with low Young's modulus values, retaining suitable mechanical strength [5]. Recently, various methods have been utilized to enhance the osseointegration of titanium dental implants. These methods are mainly based on surface, chemical or physical modifications [6]. Among them, acid etching was the one used. The main goal of physical modifications of the surface of Ti and Ti alloy implants is the creation of micro and nanostructures to stimulate osseointegration [6, 7] by increasing the porosity for cell adhesion and proliferation or adapting roughness to better wettability, protein adsorption, and bactericidal response. Furthermore, the high roughness in terms of patterned surfaces is also suitable for preventing bacterial growth colonization. The main objective of this research work is the design, manufacture, characterization, and machining of a dental implant with longitudinal porosity by PM and spacers route.

2 Materials and Methods

Commercially pure titanium (c.p. Ti) powder produced by a hydrogenation/dehydrogenation process has been used as the starting powder (SE-JONG Materials Co. Ltd., Incheon, Korea). Its chemical composition is equivalent to c.p. Ti ASTM F67–00 Grade IV. Ammonium bicarbonate has been used as space holders (Alfa Aesar, with a purity of 99.9%). NH_4HCO_3 particles with a size range of 100 to 200 μm were chosen to prepare the porous mixture with c.p. Ti. Figure 1 shows the sequence of steps for the fabrication, characterization, and machining of dental implants. For the fabrication of the dental implant preform by conventional PM and SH techniques, first, Ti powders, and a blend of c.p. Ti and 30 vol% of spacer particles were homogenized in a Turbula® T2C Shaker-Mixer for 40 min, respectively. Then, the mixtures were uniaxially pressed in a cylindrical die (8 mm of diameter) using an Instron 5505 universal testing machine (Instron, High Wycombe, U.K.), at 800 MPa, according to the compressibility curve of the material. Afterwards, the elimination of SH particles was completed. The NH_4HCO_3 was thermally removed (60 °C and 110 °C; both stages of the thermal treatment are carried out for 10–12 h and at low vacuum conditions 10^{-2} mbar) [4]. Sintering was carried out in a molybdenum chamber furnace (Termolab, Agueda, Portugal) under high vacuum conditions ($\sim 10^{-5}$ mbar) at 1523 K for 2 h. To evaluate the structural integrity and interface quality, images of the preforms were captured after compaction (green preforms) and after sintering.

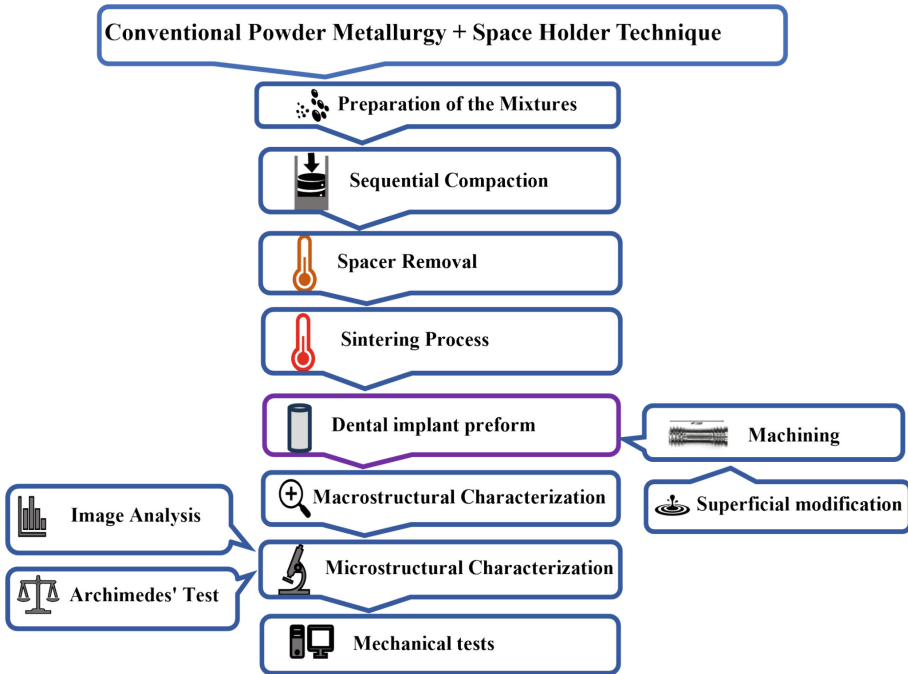


Fig. 1. Sequence of steps for the fabrication, characterization, and machining of dental implants.

Moreover, the sintered preform was cut transversely for microstructural characterization. Archimedes' Test [8] was employed to determine the percentage of total (P_T) and interconnected porosity (P_i), from the density measurement. In addition, total porosity, equivalent diameter, D_{eq} , and shape factor (F_f , ratio between major and minor axis of an ellipse equivalent to pore) and fraction volume (P_T) were evaluated by image analysis (IA), using an optical microscope Nikon Epiphot (Nikon, Tokyo, Japan) coupled with a camera Jenoptik Progres C3 (Jenoptik, Jena, Germany) and results were analyzed using NIS-Elements software. Image analysis (IA) was performed using five pictures of 5X magnification. Micro-tribomechanical behavior of the samples was evaluated by instrumented micro-indentation (P - h curves) and scratch tests. Loading-unloading tests were performed using a Microtest machine (MTR3/50-50/NI) equipped with a Vickers indenter, at an applied load rate of 5 N/min, a maximal load of 5 N and a holding time of 15s. Indentations were performed in three different regions of the preform. Scratch test was performed on the surface of the cross section of the sintered preform using a MICROTTEST commercial device (MTR3/50-50/NI) with a Rockwell diamond tip of 200 μm diameter applying a maximum constant load of 3 N at a rate of 1 mm min^{-1} for 11 mm of scar length, following the ASTM C1624-05 standard [9]. A cylindrical preform was micromachined using a Numerical Control Center (CNC) milling machine (Roland, Model MDX-40) until obtaining the designed dental implant. The following sequence of operations were used: turning, threading of the ends, milling of the bone

cutting grooves, grinding, polishing of the porous zone, and finally punching. Superficial modifications were implemented to enhance the osseointegration capacity of the implants. Three micro-machined implants were subjected to surface modification in the apex region using hydrofluoric acid solutions with varying concentrations of inhibitor. Three different times of exposition were used, 15 s; 60 s and 125 s. Prior to surface modification, the surfaces of the samples were successively ultrasonically cleaned in acetone (15 min), alcohol (20 min) and distilled water (20 min).

3 Results and Discussion

As depicted in Fig. 2, the dental implant preform design includes a top region (direct contact with the oral cavity), and an apical region (in contact with the alveolar bone), both composed of dense c.p. Ti, the central porous section is a combination of c.p. Ti and spacer particles of NH_4HCO_3 .

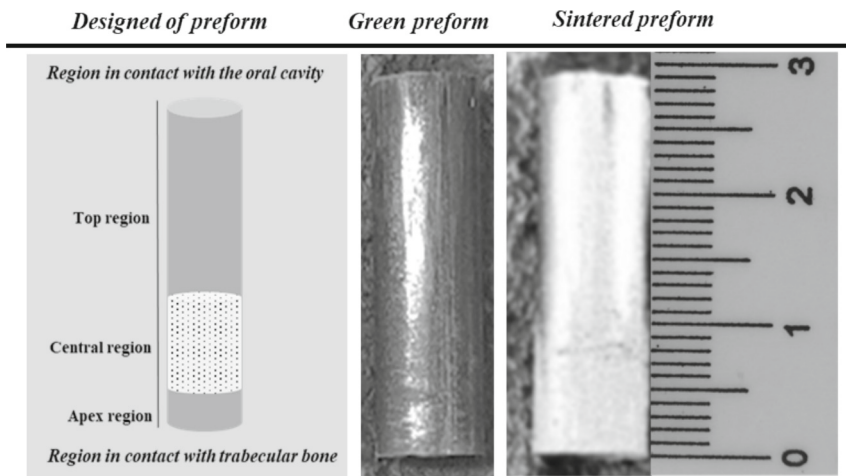


Fig. 2. Design, green and sintered preform for fabrication of dental implant.

The dimensions of the sintered preforms validate the design and suitability of manufacturing process. A cylindrical preform with a diameter of 8.0 mm and a length of 30 mm was achieved. Green preforms appear as opaque dark grey, while sintered preforms have a clean, shiny appearance.

The cross section of sintered preform is shown in Fig. 3, with details of achieve longitudinal porosity of each zone. Two types of porosity could be observed, on the one hand, the conventional microporosity related to the PM manufacturing process (apex region and top region), and on the other hand, the microporosity (porous region) due to the spacer particles. The optical microscope images reveal that a longitudinal porosity gradient has been accomplished. The length of apex and porous region are approximately 3.0 mm and 6.0 mm, respectively, in accordance with the designed preform. The upper

region is close to 21 mm since this zone was designed to assist the posterior micromachining process. The porous region is delimited irregularly with dense regions, possibly due to the compacting of the powders during final distribution. The central region has non-homogeneous porosity.

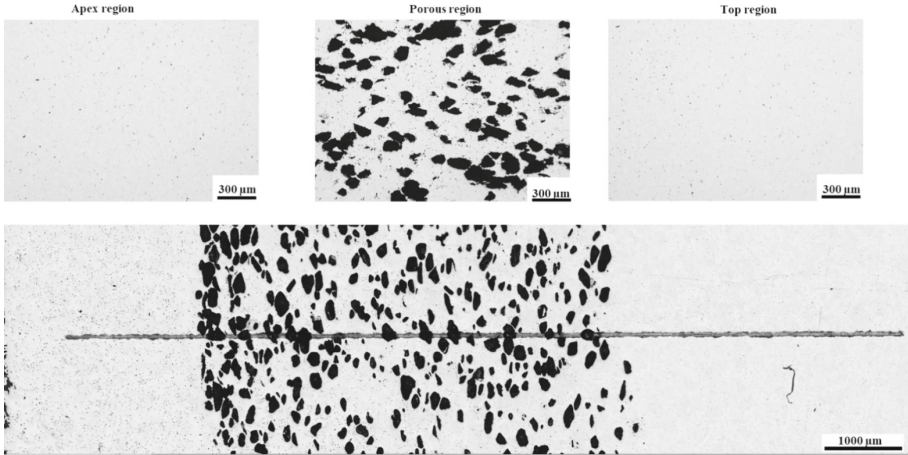


Fig. 3. Optical images of the three regions of sintered preform and cross section of the preform.

Results of IA and Archimedes test are summarized in Table 1. The top and apex regions exhibit similar total porosity by Archimedes (10.6% and 10.0% respectively); however, these values of porosity could be influenced by imprecise cutting of the preform, due to its small dimensions and irregular porous/dense interfaces. By contrast, total porosity (P_T) obtained by IA is in accordance with expected higher porosity of apex region compared to top region, (3.32 vs.1.03%). Furthermore, the apex and upper region showed different equivalent diameters values of $3.6 \mu\text{m}$ and $2.7 \mu\text{m}$ respectively. Finally, the shape factor parameter revealed similar results for both regions.

Table 1. Results of IA and Archimedes' Test of the sintered preform.

Regions	Archimedes' Test		Imagen analysis		
	P_t [%]	P_i [%]	P_T [%]	$D_{eq}[\mu\text{m}]$	F_f
Top	10.6 ± 1.8	8.8 ± 1.8	1.03 ± 0.2	2.7 ± 0.04	0.77 ± 0.01
Central	24.4 ± 5.2	10.0 ± 5.9	26.0 ± 3.8	118.4 ± 9.5	0.44 ± 0.03
Apex	10.0 ± 8.8	5.7 ± 9.1	3.32 ± 0.2	3.6 ± 0.5	0.78 ± 0.01

On the other hand, results by IA from the porous zone revealed that the geometry of pores (F_f), the equivalent diameter (D_{eq}), and surface porosity (P_T) were in accordance with the size of spacer particles used to generate porosity [5]. The equivalent pore diameter of $118.4 \mu\text{m}$ could promote bone ingrowth into the dental implant [10].

Further characterization of porosity was achieved using the Archimedes' Test, including total and interconnected porosity. Total porosity of porous zone was 24.4% by volume, which is close to the proposed volume content of 30%. Additionally, interconnected porosity of 10.0% could promote cell growth. Furthermore, the pores are elongated showing a shape factor of 0.44.

These characteristic manufactured Ti scaffold containing a variety of small and large pores with diverse shapes, could be advantageous to allow the osteoblasts to proliferate and differentiate [11].

Tribo-mechanical tests were performed on the polished cross section of sintered preform. Figure 4 shows the scratch of the dental implant, from the dense apex region, passing through the porous region and ending in the top region (11.0 mm). The increase of roughness in the central porous region, with respect to the dense zones, is clearly shown.

The optical microscopy images, see Fig. 4 illustrate details of the dragging of the material during scratching, with a focus on the porous region. These values indicate a lower hardness of the porous zone and therefore a lower Young's modulus.

The elastic recovery capacity of the preform zones is shown in Table 2. As expected, the porous region has better elastic recovery capacity compared to apical and top region.

Table 2. Elastic recovery of the dental implant.

Regions	Penetration depth (μm)		Elastic Recovery Absolut (μm)
	Maximum	Permanent (unloaded)	
Top and Apex	2.90	1.88	1.03
Porous	3.19	1.83	1.36

In Fig. 5 details of micromachined dental implant are shown, starting from the design provided by SOLIDWORKS 3D CAD software. Dental implant was created by machining the sintered preform according to the following steps: turning, threading of the ends, milling of the bone cutting grooves, grinding, polishing of the porous surface, and finally punching. For this purpose, a CNC lathe and a milling machine was employed. As a result, dental implant is provided with two external threads located in the apical and superior regions respectively. Apical thread includes a bone-cutting groove. On the other hand, the dental implant has an internal hexagonal thread, in which the prosthetic rehabilitation will be located. Figure 5 also shows a summary sequence of steps followed by the dental implant preform up to machining, the images display the implant before and after it was cut. Additionally, image of the lower thread etched with fluorhydric acid at 50 °C for 125 s of exposure is illustrated (Fig. 5). Acid etched apex zone has resulted in the presence of an increased roughness, that would facilitate the adhesion of osteoblastic cells and promotes osseointegration of the device.

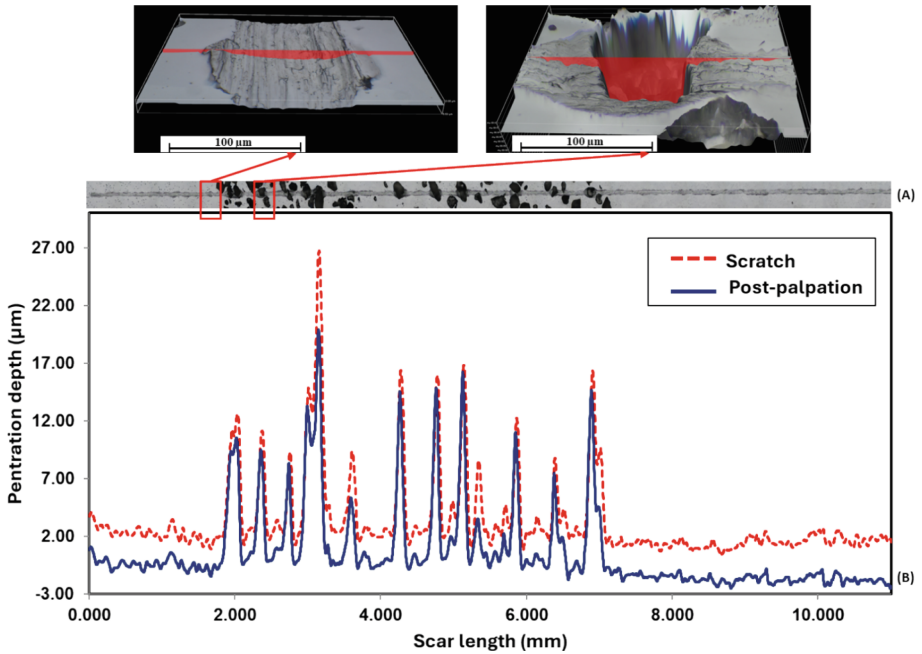


Fig. 4. Scratch test: (A) Optical image of scar, with zoom out of two highlighted zones, and (B) Scratch profile with maximum penetration depth and elastic recovery after scratch test.

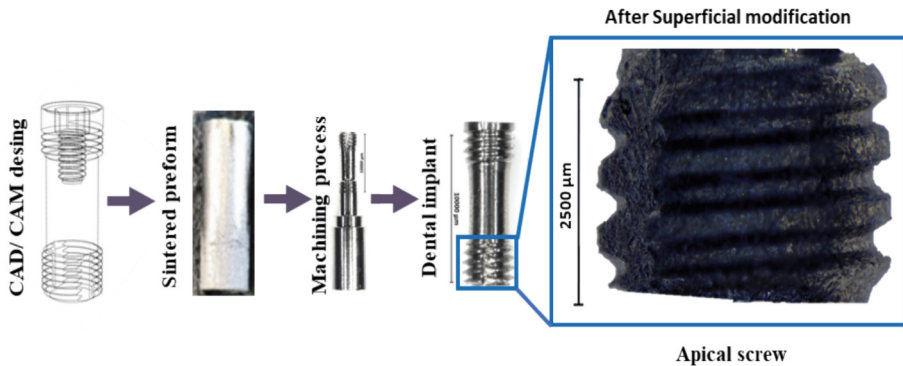


Fig. 5. Overview of dental implant manufacture from CAD/CAM design, sintered cylindrical preform to final micromachined dental implant, and surface modification of the apical zone of the dental implant.

4 Conclusion

The results corroborate and reaffirm Powder Metallurgy as an important method for the manufacture of devices for bone replacements using c.p. Ti. The design and manufacturing process used to obtain the dental implant is feasible. The volumetric porosity and pore size range obtained are consistent with the design. The dimensions of the sintered

perform ensure successful machining. Hardness tests demonstrate a reduction in the Young's modulus of the device, which would promote osseointegration. The chemical treatment carried out in the apical area increases the roughness of the surface, potentially improving successful osseointegration of the implant.

Acknowledgments. This work was supported by the Spanish Ministry of Science and Innovation through the R+D+i project grant PDC2022-133369-I00. Danaysi Mena extends her sincere thanks to the Junta de Andalucía, Consejería de Transformación Económica, Industria, Conocimiento y Universidades, for their support through the Predoctoral Contract PAIDI 2021, file number PREDOC_00694. Technical assistance provided from J. Pinto in tribomechanical testing and J.M. Jaramillo in the machining of the dental implant is also acknowledged.

References

1. Torres, Y., Trueba, P., Pavón, J., Montealegre, I., Rodríguez-Ortiz, J.A.: Designing, processing and characterisation of titanium cylinders with graded porosity: an alternative to stress-shielding solutions. *Mater. Design* **63**, 316–324 (2014). <https://doi.org/10.1016/j.matdes.2014.06.012>
2. Niinomi, M., Nakai, M., Hieda, J.: Development of new metallic alloys for biomedical applications. *Acta Biomater.* **8**(11), 3888–3903 (2012). <https://doi.org/10.1016/j.actbio.2012.06.037>
3. Norowski, P.A., Jr., Bumgardner, J.D.: Biomaterial and antibiotic strategies for periimplantitis: a review. *J. Biomed. Mater. Res. Part B: Appl. Biomater.: Off. J. Soc. Biomater. Jpn. Soc. Biomater. Aust. Soc. Biomater. Korean Soc. Biomater.* **88**(2), 530–543 (2009). <https://doi.org/10.1002/jbm.b.31152>
4. Torres, Y., et al.: Processing, characterization and biological testing of porous titanium obtained by space-holder technique. *J. Mater. Sci.* **47**(18), 6565–6576 (2012). <https://doi.org/10.1007/s10853-012-6586-9>
5. Lascano, S. et al.: Porous titanium for biomedical applications: evaluation of the conventional powder metallurgy frontier and space-holder technique. *Appl. Sci.* **9**(5) (2019). <https://doi.org/10.3390/app9050982>
6. Wennerberg, A., Albrektsson, T.: Effects of titanium surface topography on bone integration: a systematic review. *Clin. Oral Implants Res.* **20**(Suppl 4), 172–184 (2009). <https://doi.org/10.1111/j.1600-0501.2009.01775.x>
7. Trueba, P., Navarro, C., Rodríguez-Ortiz, J.A., Beltrán, A.M., García-García, F.J., Torres, Y.: Fabrication and characterization of superficially modified porous dental implants. *Surf. Coatings Technol.* **408**, Art no. 126796 (2021). <https://doi.org/10.1016/j.surfcoat.2020.126796>
8. ASTM International ASTM C373-14, Standard Test Method for Water Absorption Bulk Density, Apparent Porosity and Apparent Specific Gravity of Fired Whiteware Products; International, A., Ed. (2014). <https://doi.org/10.1520/C0373-14>
9. ASTM C1624-05 Standard Test Method for Adhesion Strength and Mechanical Failure Modes of Ceramic Coatings by Quantitative Single Point Scratch Testing 2015, ASTM International, West Conshohocken, PA (2015). <https://doi.org/10.1520/C1624-05R15>
10. Frosch, K.-H., et al.: Growth behavior, matrix production, and gene expression of human osteoblasts in defined cylindrical titanium channels. *J. Biomed. Mater. Res. Part A* **68A**(2), 325–334 (2004). <https://doi.org/10.1002/jbm.a.20010>
11. Liang, H., et al.: Trabecular-like Ti-6Al-4V scaffolds for orthopedic: fabrication by selective laser melting and in vitro biocompatibility. *J. Mater. Sci. Technol.* **35**(7), 1284–1297 (2019). <https://doi.org/10.1016/j.jmst.2019.01.012>